

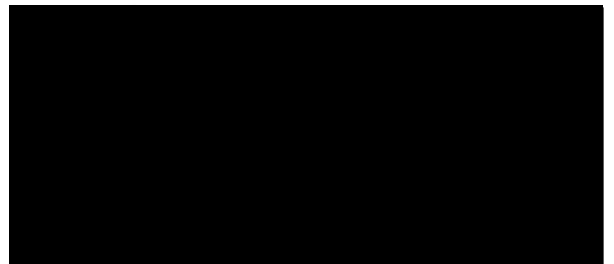
WSRC-TR-2004-00580 (U)

***Galvanic Corrosion in Waste Tank Environments
(U)***

B. J. Wiersma

J. I. Mickalonis

Savannah River National Laboratory
Strategic Material Technology Department
Materials Technology Section



Publication Date: December 2004

**Westinghouse Savannah River Company
Savannah River Site
Aiken, SC 29808**

This document was prepared in connection with work done under Contract No. DE-AC09-96SR18500 with the U. S. Department of Energy

DISCLAIMER

This report was prepared as an account of work sponsored by an agency of the United States Government. Neither the United States Government nor any agency thereof, nor any of their employees, makes any warranty, express or implied, or assumes any legal liability or responsibility for the accuracy, completeness, or usefulness of any information, apparatus, product, or process disclosed, or represents that its use would not infringe privately owned rights. Reference herein to any specific commercial product, process, or service by trade name, trademark, manufacturer, or otherwise does not necessarily constitute or imply its endorsement, recommendation, or favoring by the United States Government or any agency thereof. The views and opinions of authors expressed herein do not necessarily state or reflect those of the United States Government or any agency thereof.

WSRC-TR-2004-00580

SMTD

Strategic Materials Technology Department

Keywords: Corrosion,
Chemistry, Waste Tank

Retention - Permanent

Galvanic Corrosion in Waste Tank Environments

by

B. J. Wiersma

and

J. I. Mickalonis

SRNL

SAVANNAH RIVER NATIONAL LABORATORY, AIKEN, SC 29808

Westinghouse Savannah River Company

Prepared for the U. S. Department of Energy under Contract DE-AC09-96SR18500

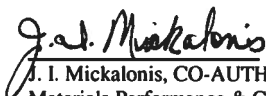
APPROVALS

WSRC-TR-2003-00580



Date: 12-2-04

B. J. Wiersma, CO-AUTHOR
Materials Performance & Corrosion Technology Group
MATERIALS TECHNOLOGY SECTION



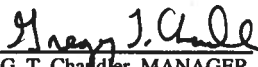
Date: 12/3/04

J. I. Mickalonis, CO-AUTHOR
Materials Performance & Corrosion Technology Group
MATERIALS TECHNOLOGY SECTION



Date: 12-2-04

P. E. Zapp, TECHNICAL REVIEWER
Materials Performance & Corrosion Technology Group
MATERIALS TECHNOLOGY SECTION



Date: 12/2/04

G. T. Chandler, MANAGER
Materials Performance and Corrosion Technology Group
MATERIALS TECHNOLOGY SECTION



Date: 12/8/04

T. M. Punch, CUSTOMER
TCP & WOW Engineering *BJW*



Date: 12-13-04

E. J. Freed, MANAGER
H & F Process Support

Galvanic Corrosion in Waste Tank Environments

1.0 Summary

The Closure Business Unit plans to utilize a submersible mixer pump during bulk sludge removal operations in waste tanks. The foot of the pump will rest on the bottom of the tank. The foot of the pump is constructed of stainless steel, while the tank bottom is constructed of carbon steel. The risk of accelerated attack due to contact between dissimilar metals (i.e., galvanic corrosion) was assessed.

Laboratory data relevant to the carbon steel/stainless steel couple that has been exposed to a simulated waste environment was reviewed. The data indicated that either the carbon steel tank or the stainless steel foot may be the anode (i.e., component that corrodes). However, the corrosion rates of both materials were estimated to be less than 1 mpy. Thus the severity of the attack on either of these materials is expected to be minor.

2.0 Background

The Closure Business Unit plans to utilize a submersible mixer pump (SMP) during bulk sludge removal operations in waste tanks [1]. The foot of the pump will rest on the bottom of the tank (See Figure 1 for drawing of foot). The foot of the pump is constructed of stainless steel, while the tank bottom is constructed of carbon steel.

Contact between dissimilar metals has the possibility of accelerating the corrosion rate of the more active material. This type of corrosion is referred to as galvanic. Galvanic corrosion is driven by the potential difference of the two metals in a given environment. The severity of galvanic corrosion is governed by several factors including the equilibrium corrosion potential (E_{corr}), their polarization characteristics, the solution resistance, and the area ratio between anodic and cathodic regions. The available corrosion data for stainless steel and carbon steel in waste simulants will be evaluated and applied to this specific case.

For a particular solution, a metal has an E_{corr} that develops from the interaction of the metal surface with the environment. Corrosion potentials for metals in a particular environment may be listed in numerical order. This listing is referred to as a galvanic series. The galvanic series may be utilized to determine the initial relationship of two dissimilar metals that are in contact. The metal with the more electro-negative potential (i.e., more active) will be the anode of the galvanic couple, while the metal with the more electro-positive potential will be the cathode.

The initial relationship between the dissimilar metals may change depending on the magnitude of the difference between their E_{corr} values. For a large difference, the initial relationship will likely remain unchanged over time. However, a small difference may

result in a relationship in which the anode alternates between the two metal or completely switches from one metal to the other.

A significant factor in the severity of attack is the area ratio of the anodic to cathodic regions. The galvanic current density (I_{couple}) which is proportional to the galvanic corrosion rate is an area-dependent variable. All of the electrochemical galvanic corrosion testing at SRS has been performed with a cathode to anode area ratio of 1:1. The galvanic corrosion rate will generally decrease as the cathode to anode area ratio decreases below 1:1. Conversely, if the cathode to anode area increases above 1:1, the severity of attack will also increase. This area dependence assumes that the corrosion process is under cathodic control. For these materials in the waste environments this is a reasonable assumption.

3.0 Evaluation of Stainless Steel/Carbon Steel Galvanic Corrosion Data

3.1 Electrochemical Data

3.1.1 Waste Simulant Solutions and Material Conditions

The composition of the waste during bulk sludge removal can range from a concentrated supernate (i.e., nitrate, nitrite, or hydroxide greater than 1 M) to a rather dilute solution due to the addition of water as the slurry medium. Operation of the SMP may also raise the temperature of the waste due to dissipation of mechanical energy. Thus galvanic corrosion data that spans a fairly wide range of compositions and temperatures should be evaluated.

Galvanic corrosion rate data for the carbon steel/stainless steel couple was obtained for the ten solutions shown in Table 1 [2, 3]. Based on previous sludge removal operations [4, 5] these compositions appear to bracket the waste compositions that may be expected during bulk sludge removal. It should be noted that pitting of carbon steel has been observed during corrosion tests in waste simulants # 2, 5, and 8. This result was expected as the test solutions do not meet the minimum nitrite requirement specified by the Corrosion Control Program [6]. Waste simulant #7 also does not meet the minimum nitrite requirement specified. Although no pits were observed on the carbon steel sample following the electrochemical test, the results of the test suggest that the passive film is experiencing some activity [7]. It is recommended that the sludge slurry not be allowed to achieve these low inhibitor levels as this may impact other tanks downstream that receive the sludge slurry transfer as well as the tank in which removal is being performed.

The tests were performed at temperatures of 30, 45, and 60 °C. The initial temperature of the supernate above sludges tends to be between 30 to 45 °C, while the initial sludge temperatures tend to be between 30 to 74 °C [8]. The temperature of the sludge frequently depends on the availability of the cooling coils in the tank. As mentioned earlier the SMP will likely raise the temperature slightly in the tank. Although no detailed energy balance calculations have been performed, the temperature of the sludge slurry in most cases of bulk removal is expected to be within the range of the test data.

The materials utilized for the corrosion tests were 304L stainless steel (304L) and A537 Class I carbon steel (A537). Additional 304L samples were heat treated (304L-ht) at 650 °C for 24 hours. These samples were prepared to simulate base metal that had been exposed to high temperatures during welding processes. Prior to performing each electrochemical test, the samples were polished to a 600 grit finish to ensure a uniform surface for testing.

3.1.2 Variability in E_{corr} Measurements

The E_{corr} value for 304L and A537 exposed to these environments was monitored for time periods ranging between 30 minutes and 48 hours. For both materials, E_{corr} was observed to change with time as shown in Figure 2. This data was obtained in waste simulant #9. In both cases the potential drifted in the noble, or electro-positive, direction before achieving a relatively stable value. The change in potential from the initial measurement could be as much as 100 mV. Thus the measured value of E_{corr} will depend on the time at which the measurement was taken.

The value of E_{corr} may also vary even if the measurements are taken at the same time. Figure 3 shows results of E_{corr} measurements for 304L and A537 obtained after 30 minutes of exposure to waste simulant #6 at 30 °C. As can be seen from the figure the tests were performed on different days. Thus different batches of the same solution were utilized, as well as different samples of the same material. For 304L the average value for E_{corr} was -433 mV, the standard deviation was approximately 44 mV and the range was between -350 mV to -500 mV. These differences may be attributed to slight changes in the solution environment, differences in handling the samples during surface preparation, and differences in the microstructure of the material that is exposed at the surface. Although there are fewer data points, the variability in E_{corr} for A537 exposed to the same environment for 30 minutes appears to be similar to the 304L.

The E_{corr} values for 304L and A537 in the same environment are relatively close despite the variability. Figure 2 shows that the two potentials are within 20 mV at all times. Figure 3 shows that both of the E_{corr} values for carbon steel were within the range of E_{corr} values measured for the stainless steel. The relative closeness of the E_{corr} values in other waste simulants will be examined in section 3.1.3. As a consequence of these observations, either the stainless steel or carbon steel may be the anode in the coupled system. The fact that E_{corr} for both materials changes with time also means that the material that behaves like the anode could change with time. The relative closeness of the E_{corr} values also suggests that the galvanic current between the two materials may be small. This assessment will be confirmed in section 3.1.4 when the polarization characteristics of these two materials in these environments are evaluated.

3.1.3 E_{corr} Values in Waste Simulants

Table 2 shows the values measured for E_{corr} in the various waste simulants. E_{corr} values for the first 8 simulants were measured after 30 minutes, while the E_{corr} values for

simulants # 9 and 10 were monitored for up to 2 days. In most simulants, the E_{corr} values for A537 were anodic to those for 304L and 304L-ht. The differences in potential ranged from 2 to 125 mV. Thus at least initially A537 is likely to be the anode in most waste environments. However, the variables mentioned in section 3.1.2 could easily result in the 304L materials becoming the anode. These differences in potential are small and should result in a small galvanic current.

The table also shows that the potential differences between 304L and 304L-ht couple are also small. The data is not conclusive as to which material would be the anode. The data appears to suggest that at a low simulant temperature 304L-ht is the anode, while at the higher temperature 304L appears to be the anode. The mechanistic explanation for this observation is unknown at this time.

3.1.4 Estimation of Corrosion Rates

3.1.4.1 Corrosion Rates of Stainless Steel and Carbon Steel in Waste Simulants

The corrosion rates of 304L and A537 by themselves in each of the environments were determined by two methods. Tafel slope measurements [9] were utilized to determine the corrosion rates in simulants #9 and 10. For these tests, the potential was initially polarized 200 mV below E_{corr} . The potential was then increased to a value 200 mV above E_{corr} while the current is measured (see Figure 4). The portion of the curve where the potential is below E_{corr} is referred to as the cathodic branch while the portion above E_{corr} is referred to as the anodic branch. Tangent lines are drawn to the cathodic and anodic branches of the plots. The two lines intersect at E_{corr} at a current value known as I_{corr} . I_{corr} is proportional to the corrosion rate of the material as given by equation 1 [10].

$$\text{Corrosion Rate} = \frac{0.13 * (\text{Equivalent Weight of Corroding Species}) * I_{\text{corr}}}{(\text{Density of the Material})} \quad (1)$$

For both 304L and A537 the corroding species is iron, thus the equivalent weight is 27.4 g/equivalent and the density is approximately 7.9 g/cm³. Table 3 shows the values for I_{corr} and the corrosion rate for A537 and 304L in simulants #9 and 10. The corrosion rates are less than 1 mpy.

The data for simulants #1 through 8 were obtained from anodic cyclic polarization (CP) scan [11]. Figure 4 shows an example of a typical CP curve for A537 in these waste simulants. The scan is initiated at 50 mV below E_{corr} . The potential is increased until a breakdown potential (i.e., location where current increases significantly with little change in the potential) occurs and then the potential is returned to the initial E_{corr} value. The anodic branch of the curve is characterized by a region where the value of the current density does not change with potential. This behavior is due to the presence of a passive oxide film on the surface of the material. This current density is commonly referred to as the passive current density (I_p). As shown in Figure 4, I_p is clearly greater than I_{corr} . Therefore as a conservative estimate for the corrosion rate I_p may be substituted into

equation (1) for I_{corr} . Values for I_p and the corrosion rate for A537 and 304L in simulants #1 through 8 are shown in Table 4. The corrosion rates are less than 1 mpy.

3.1.4.2 Galvanic Corrosion Rates for Stainless Steel and Carbon Steel in Waste Simulants

Galvanic corrosion rates were measured by one of two techniques: 1) Direct galvanic current measurement, 2) a Tafel slope overlay technique. In the tests that were performed the areas of the A537 and 304L samples were equal. Direct galvanic current measurement [12] was performed by immersing both materials in the test solution and then connecting them both to an external zero resistance ammeter that will measure the current (I_{couple}) that is passed between them as a function of time (see Figure 5). In this case a negative current would mean that the carbon steel is the cathode, while a positive current would indicate that the stainless steel is the cathode. The corrosion rate may be estimated by substituting I_{couple} for I_{corr} in equation 1.

Figure 6 shows an example of the Tafel slope overlay technique [13]. The Tafel curves for A537 and 304L in simulant #9 were plotted together. In this case, A537 is anodic to 304L. The I_{couple} is determined by the intersection of the anodic branch of the A537 curve and the cathodic branch of the 304L curve. At this potential the anodic current density equals the cathodic current density. Note that since the potentials are so close together, very little polarization of either surface occurs. As a result a small galvanic current density would be anticipated.

Direct galvanic current measurements were performed in simulants #9 and 10. Figure 4 shows I_{couple} as a function of time for simulant #10. The test was initially run for 24 hours and then stopped. The test was restarted the next day and run for an additional 20 hours. Initially the carbon steel was the cathode, and the corrosion rate of the stainless steel was approximately 0.01 mpy. After approximately 10 hours, the carbon steel became the anode. At the end of 44 hours, the corrosion rate for the carbon steel was approximately 0.018 mpy. In the case of simulant #9, carbon steel remained the cathode for approximately 24 hours. At the end of 24 hours, the corrosion rate of stainless steel was approximately 0.006 mpy. Given enough time, the carbon steel may have become the anode in this solution as well. However, the corrosion rates would still be expected to be low.

The Tafel slope overlay technique was utilized for all waste simulants. The values for I_{couple} and the corrosion rate are shown in Table 5. All of the galvanic corrosion rates are less than 1 mpy. Thus the presence of the 304L/A537 galvanic couple in the waste environments does not accelerate corrosion of either metal above its normal corrosion rate. It is interesting to note that the direct galvanic current measurement indicated that stainless steel was the anode for simulant #9, whereas the overlay technique indicates that carbon steel is the anode. This observation is another example of how the anode and cathode can switch over time due to small changes in the environment or material.

3.2. Coupon Data

3.2.1 Waste Simulant Solutions and Material Conditions

Coupon tests were performed to further investigate the possibility of galvanic corrosion between A537 and 304L [2]. The compositions of the three waste simulant utilized for the coupon tests are shown in Table 6. The compositions cover a wide range of nitrate, nitrite, and hydroxide concentrations comparable to the solutions utilized for the electrochemical tests. The test temperature of the simulants was 60 °C. The A537 coupons (3/4" x 3" x 1/8") were tightly wrapped with two pieces of 304L wire. The coupon was partially immersed in the waste such that one wire was exposed to the vapor space, while the other wire was immersed. Thus, the area of the carbon steel was much greater than the area of the 304L wire. The coupons were exposed in simulant #11 for 2 months, followed by consecutive 1 month exposures in simulant #12 and #13, respectively.

3.2.2 Results of Galvanic Coupon Tests

The coupons were examined between the changes in solution. After 2 months, there was evidence of surface corrosion of the carbon steel in the vapor space, but little corrosion in the immersed region. The stainless steel wires showed no evidence of attack. No change in the appearance of the coupons was observed after 3 months. At the conclusion of the test, the coupons and wires were examined thoroughly for evidence of galvanic attack. Although a small amount of corrosion was observed, the corrosion was not associated with areas of contact between the 304L and the A537. The limited amount of corrosion observed in the coupon tests correlated well with the results of the electrochemical tests.

4.0 Application of the Galvanic Corrosion Data to the Submersible Mixing Pump

As shown in Figure 1 the diameter of the stainless steel foot of the SMP is approximately 9 inches. Thus the area of contact is approximately 64 in². Since the conductivity of the waste solution is quite high, a portion of the foot above the area in contact with the tank bottom may also be impacted. Nonetheless, the area of the stainless steel component will remain significantly less than the area of the carbon steel tank.

If the carbon steel is the anode, the corrosion rates estimated from the tests will be further reduced due to the small cathode to anode area ratio. On the other hand if the stainless steel becomes the anode, the corrosion rates will be greater than those estimated from the tests. However, given the extremely low corrosion rates when stainless steel is the anode (e.g., on the order of 0.1 mpy or less) the area ratio is not expected to play a significant factor in accelerating the corrosion. Based on the galvanic corrosion data available, no significant acceleration of corrosion is anticipated due to contact between the stainless steel foot of the SMP and the carbon steel tank.

5.0 Conclusions

Results from laboratory tests with 304L and A537 in simulated waste environments were reviewed. Galvanic corrosion due to contact between these two dissimilar metals was estimated to be less than 1 mpy. No significant acceleration of corrosion is anticipated due to contact between the stainless steel foot of the SMP and the carbon steel tank.

6.0 References

1. Drawing 6D69710, Sheet 7 of 10, Rev. 3, Mixer Pump Foot Assembly, Curtiss-Wright Electro-Mechanical Corporation, October 26, 2004.
2. J. I. Mickalonis, "Galvanic Corrosion Effects in Waste Tanks", SRT-MTS-93-3045, March 1, 1993.
3. J. I. Mickalonis, Laboratory Notebook, WSRC-NB-97-63, pp. 66-72.
4. B. J. Wiersma, "Corrosion Assessment of Bulk Waste Removal Operations in Tank 11", SRT-MTS-2004-50015, June 23, 2004.
5. B. J. Wiersma, "Corrosion Assessment of Bulk Waste Removal Operations in Tank 8", SRNL-MTS-2004-50025, October 21, 2004.
6. "CSTF Corrosion Control Program: Program Description Document", WSRC-TR-2003-00327, Rev. 3, November, 2004.
7. B. J. Wiersma, Laboratory Notebook, WSRC-NB-90-107, pp. 303-304.
8. HDP Morning Report-Waste Storage, November 17, 2004.
9. ASTM G3-89, "Standard Practice for Conventions Applicable to Electrochemical Measurements in Corrosion Testing", ASTM International, West Conshohocken, PA, 2004.
10. ASTM G102-89, "Standard Practice for Calculation of Corrosion Rates and Related Information from Electrochemical Measurements", ASTM International, West Conshohocken, PA, 2004.
11. ASTM G5-94, "Standard Reference Test Method for Making Potentiostatic and Potentiodynamic Anodic Polarization Measurements", ASTM International, West Conshohocken, PA, 1999.
12. ASTM G71-81, "Standard Guide for Conducting and Evaluating Galvanic Corrosion Tests in Electrolytes", ASTM International, West Conshohocken, PA, 2004.
13. R. G. Kelly, et al., "Electrochemical Techniques in Corrosion Engineering", University of Virginia, Charlottesville, VA, 1992.

Table 1. Major Constituents of waste simulant solutions for electrochemical tests.

Anion	Waste Simulant									
	1	2	3	4	5	6	7	8	9	10
OH ⁻	2.1	0.03	1.1	1.3	0.024	0.66	0.21	0.15	0.23	2.5
CO ₃ ⁼	0.1	0.0015	0.051	0.16	0.0023	0.081	0.14	0.098	-	-
NO ₂ ⁻	1.1	0.016	0.56	0.6	0.0085	0.3	0.1	0.07	0.09	1
NO ₃ ⁻	1.4	0.02	0.71	2	0.028	1	0.54	0.7	0.02	0.8
Cl ⁻	0.022	0.00031	0.01	0.022	0.0004	0.011	0.001	0.0013	-	-
F ⁻	0.011	0.00016	0.0056	0.015	0.00022	0.0076	-	-	-	-
SO ₄ ⁼	0.095	0.0014	0.048	0.14	0.002	0.071	0.0061	0.0079	-	-
Al(OH) ₄ ⁻	0.3	0.0043	0.15	0.31	0.0045	0.16	0.01	0.007	-	-
C ₂ O ₄ ⁼	0.0051	0.000073	0.0026	0.014	0.0029	0.0085	-	-	-	-
CrO ₄ ⁼	0.0021	0.00003	0.0011	0.0033	0.000047	0.0017	0.0012	0.00084	-	-
MoO ₄ ⁼	0.00027	0.000004	0.00014	0.00043	0.000006	0.00022	-	-	-	-
SiO ₃ ⁼	0.0021	0.00003	0.011	0.0038	0.000054	0.0019	0.00083	0.00058	-	-
PO ₄ ³⁻	0.0058	0.000084	0.0029	0.0085	0.00012	0.0043	0.02	0.014	-	-

Table 2. E_{corr} for A537 and 304L in waste simulants

Waste Simulant	Material	E_{corr} (mV vs. SCE)		
		30 °C	45 °C	60 °C
1	304L	-459		-414
	304L-HT	-467		-427
	A537	-572		-470
2	304L	-322		-250
	304L-HT	-339		-208
	A537	-405		-270
3	304L	-385		-338
	304L-HT	-393		-375
	A537	-550		-430
4	304L	-385		-409
	304L-HT	-440		-428
	A537	-510		-490
5	304L	-303		-264
	304L-HT	-304		-225
	A537	-375		-330
6	304L	-415		-395
	304L-HT	-392		-360
	A537	-470		-422
7	304L	-385		-343
	304L-HT	-420		-326
	A537	-470		-394
8	304L	-376		-351
	304L-HT	-394		-278
	A537	-445		-300
9	304L		-135	
	304L-HT			
	A537		-109	
10	304L		-345	
	304L-HT			
	A537		-347	

Table 3. Corrosion rates determined from Tafel plots.

Solution	304L Stainless Steel		A537 Carbon Steel	
	I_{corr} ($\mu A/cm^2$)	Corrosion Rate (mpy)	I_{corr} ($\mu A/cm^2$)	Corrosion Rate (mpy)
9	0.98	0.43	0.24	0.110
10	0.017	0.0077	0.53	0.24

Table 4. Corrosion rates determined from cyclic polarization plots.

Solution	304L Stainless Steel				A537 Carbon Steel			
	30 °C		60 °C		30 °C		60 °C	
	I_p ($\mu A/cm^2$)	Corrosion Rate (mpy)	I_p ($\mu A/cm^2$)	Corrosion Rate (mpy)	I_p ($\mu A/cm^2$)	Corrosion Rate (mpy)	I_p ($\mu A/cm^2$)	Corrosion Rate (mpy)
1	5.5	2.47	6.2	2.78	2.84	1.30	4.95	2.27
2	1	0.45	1.9	0.85	0.86	0.39	1.2	0.55
3	3.2	1.43	10	4.48	2.34	1.07	3.3	1.51
4	2.9	1.30	4.8	2.15	2.87	1.31	3.93	1.80
5	1.2	0.54	1.7	0.76	1.3	0.60	1.39	0.64
6	2.2	0.99	4.9	2.20	2.1	0.96	5.7	2.61
7	2.1	0.94	4.9	2.20	1.7	0.78	3.15	1.44
8	1.5	0.67	3.9	1.75	1.15	0.53	1.7	0.78

Table 5. Galvanic corrosion rates from overlay plots.

Solution	30 °C		45 °C		60 °C	
	I_{couple} ($\mu\text{A}/\text{cm}^2$)	Corrosion Rate (mpy)	I_{couple} ($\mu\text{A}/\text{cm}^2$)	Corrosion Rate (mpy)	I_{couple} ($\mu\text{A}/\text{cm}^2$)	Corrosion Rate (mpy)
1	1.0	0.46			2.0	0.92
2	0.3	0.14			0.5	0.23
3	0.5	0.23			1.0	0.46
4	0.4	0.18			0.8	0.37
5	0.3	0.14			0.5	0.23
6	0.7	0.32			1.0	0.46
7	0.5	0.23			0.8	0.37
8	0.3	0.14			0.3 ^a	0.14
9			0.055	0.03		
10			0.006 ^a	0.003		

a – Stainless steel is the anode

Table 6. Waste Simulant Compositions for Coupon Tests

	Waste Simulants		
	11	12	13
Anion			
Nitrate	1.71	0.43	0.029
Nitrite	0.51	0.13	0.0085
Hydroxide	1.4	0.35	0.023
Sulfate	0.12	0.03	0.002
Chloride	0.024	0.006	0.0004
Chromate	0.0028	0.0007	4.67E-05
Molybdate	0.00037	9.25E-05	6.17E-06
Fluoride	0.015	0.0037	0.00024

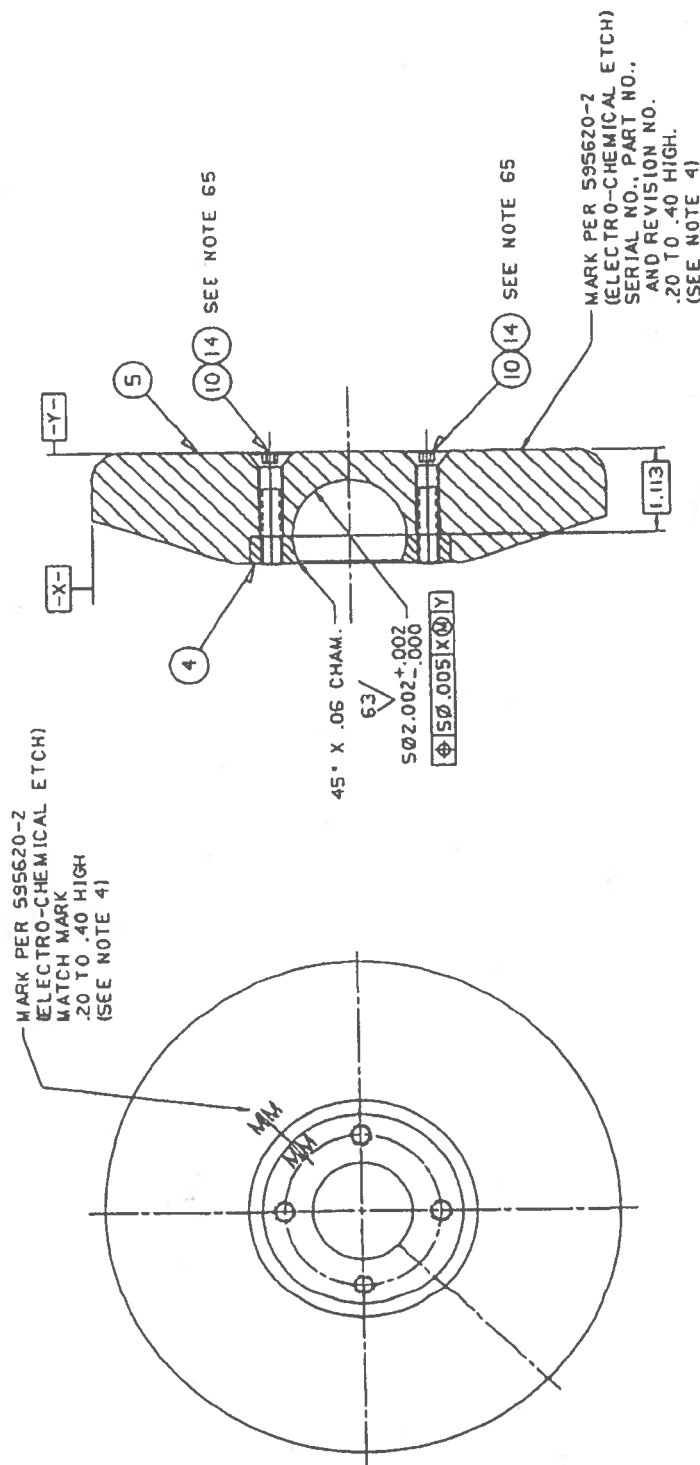


Figure 1. Submersible Mixer Pump Foot Assembly

December 2004

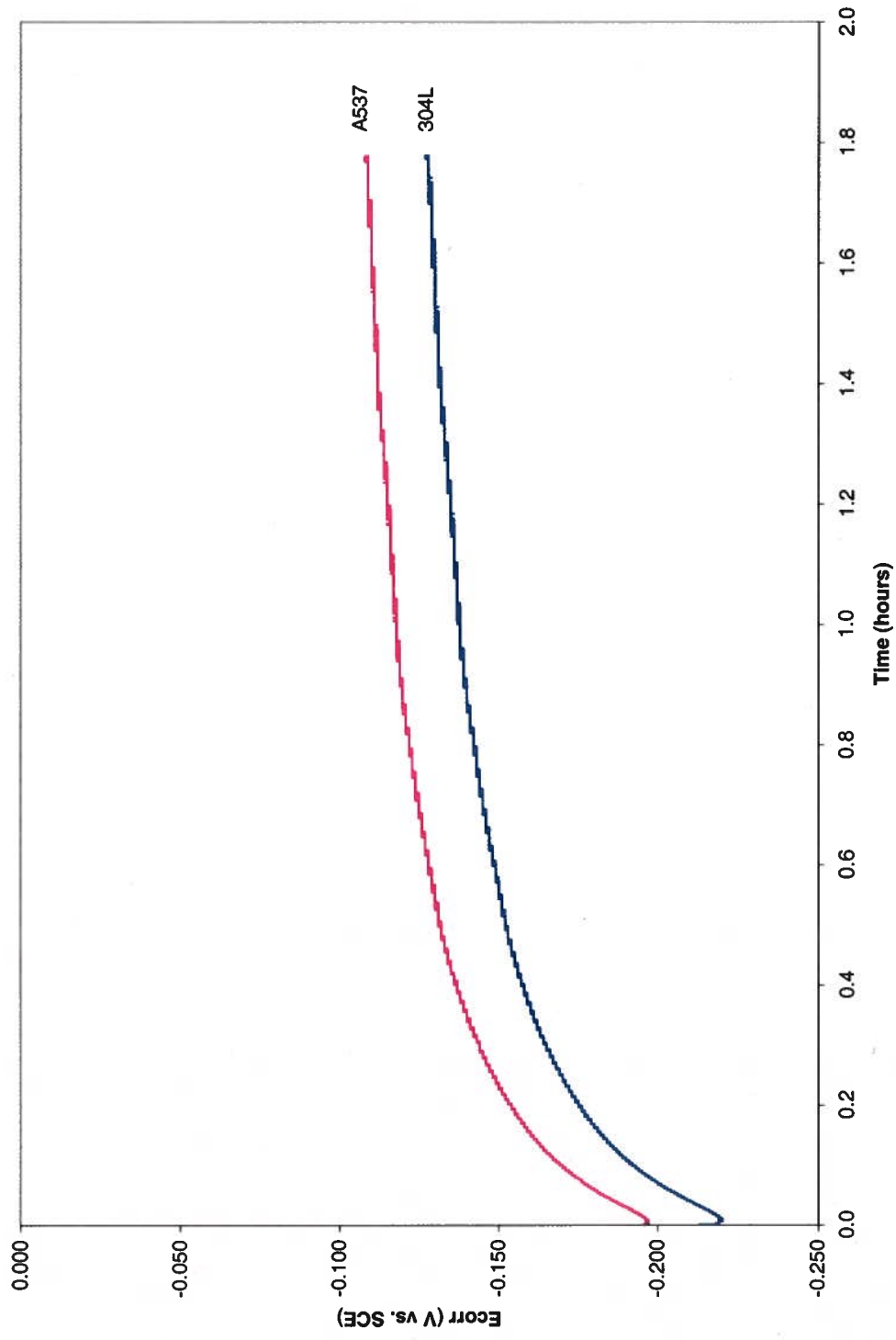


Figure 2. E_{corr} vs. time for 304L and A537 exposed to waste simulant #9.

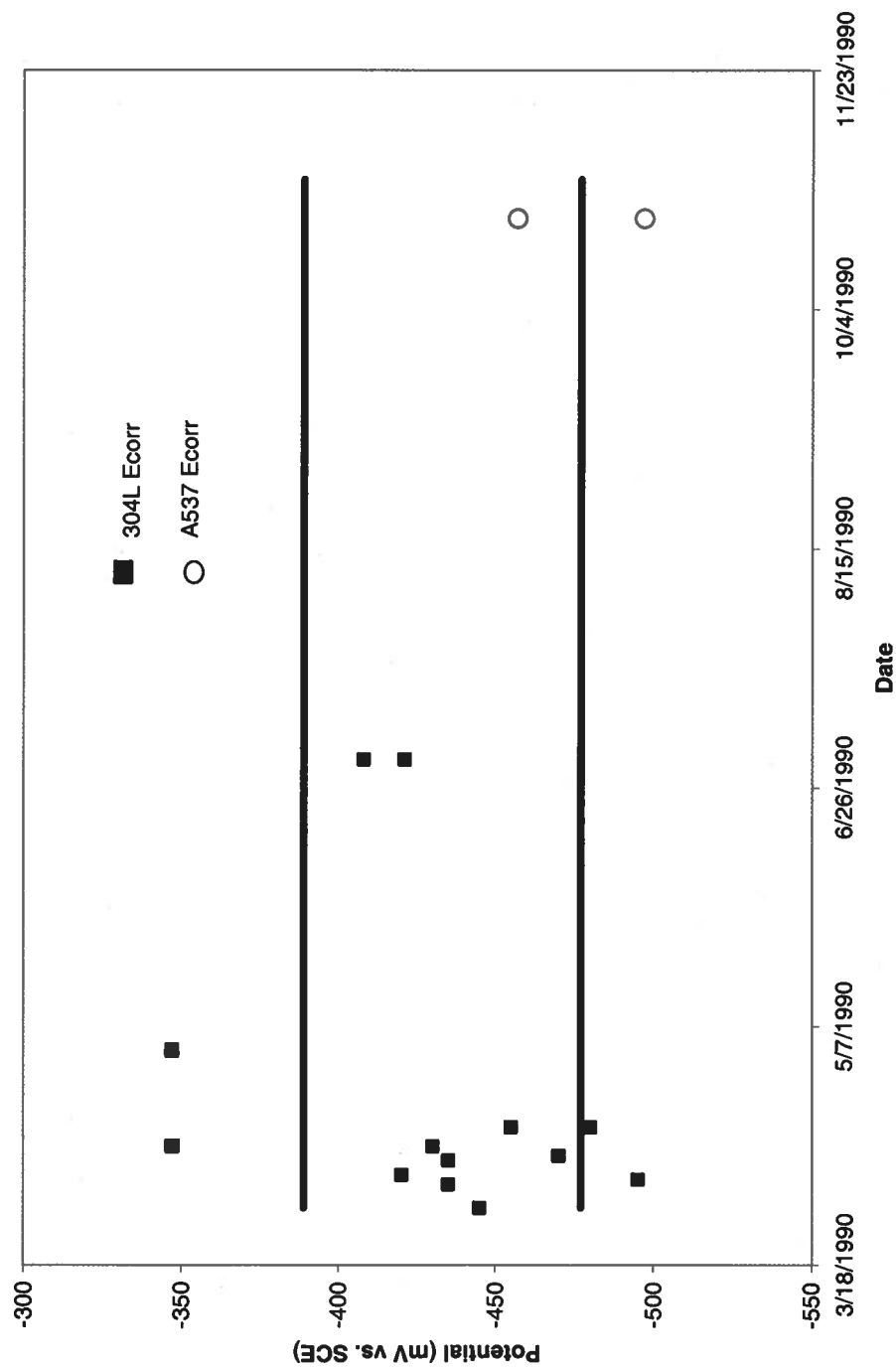
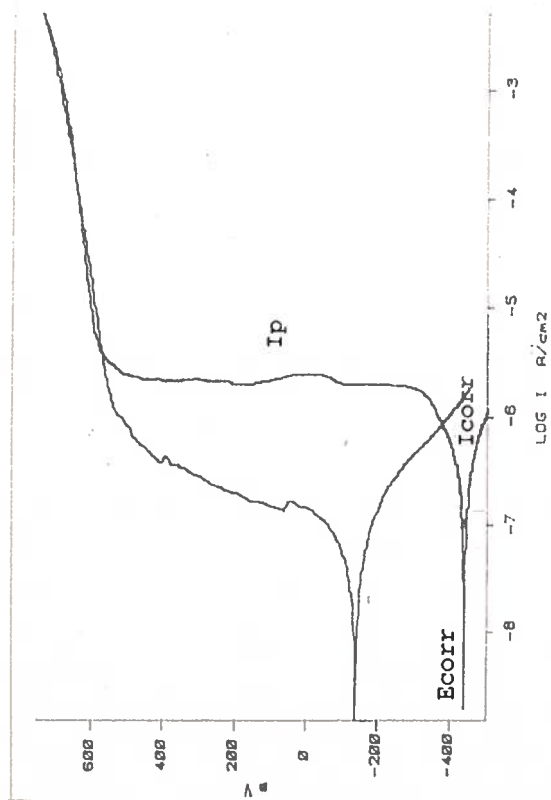
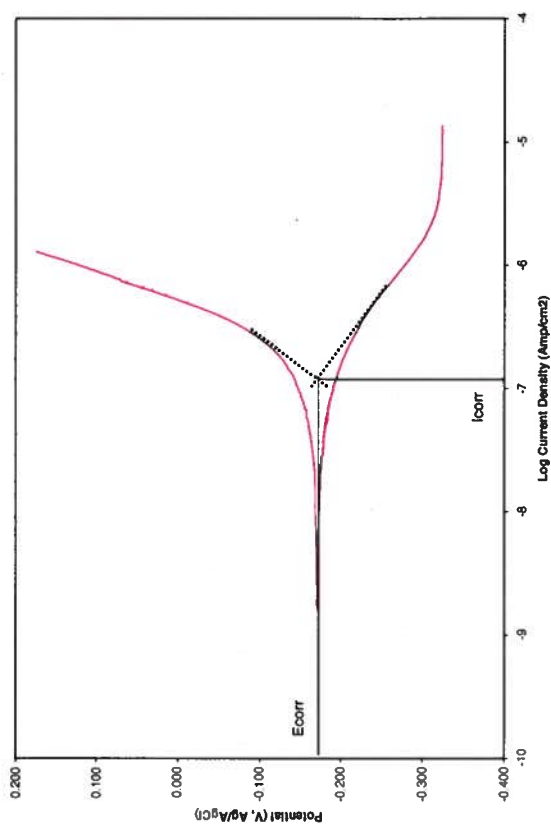


Figure 3. Variability in E_{corr} for 304L and A537 in waste simulant #6.



(a)



(b)

Figure 4. Examples of a) Cyclic Polarization and b) Tafel plots

December 2004

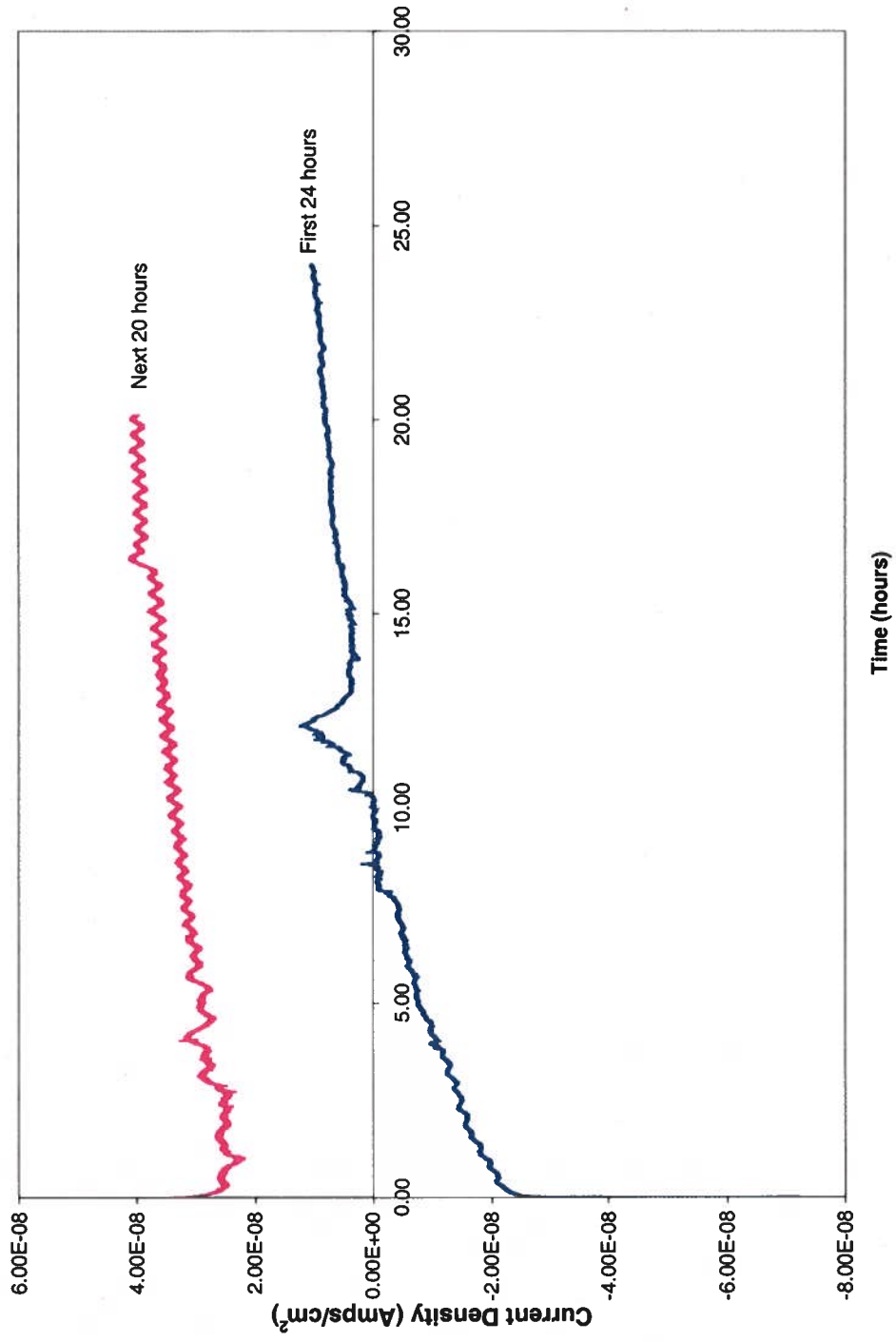


Figure 5. Direct galvanic current measurement in waste simulant #10.

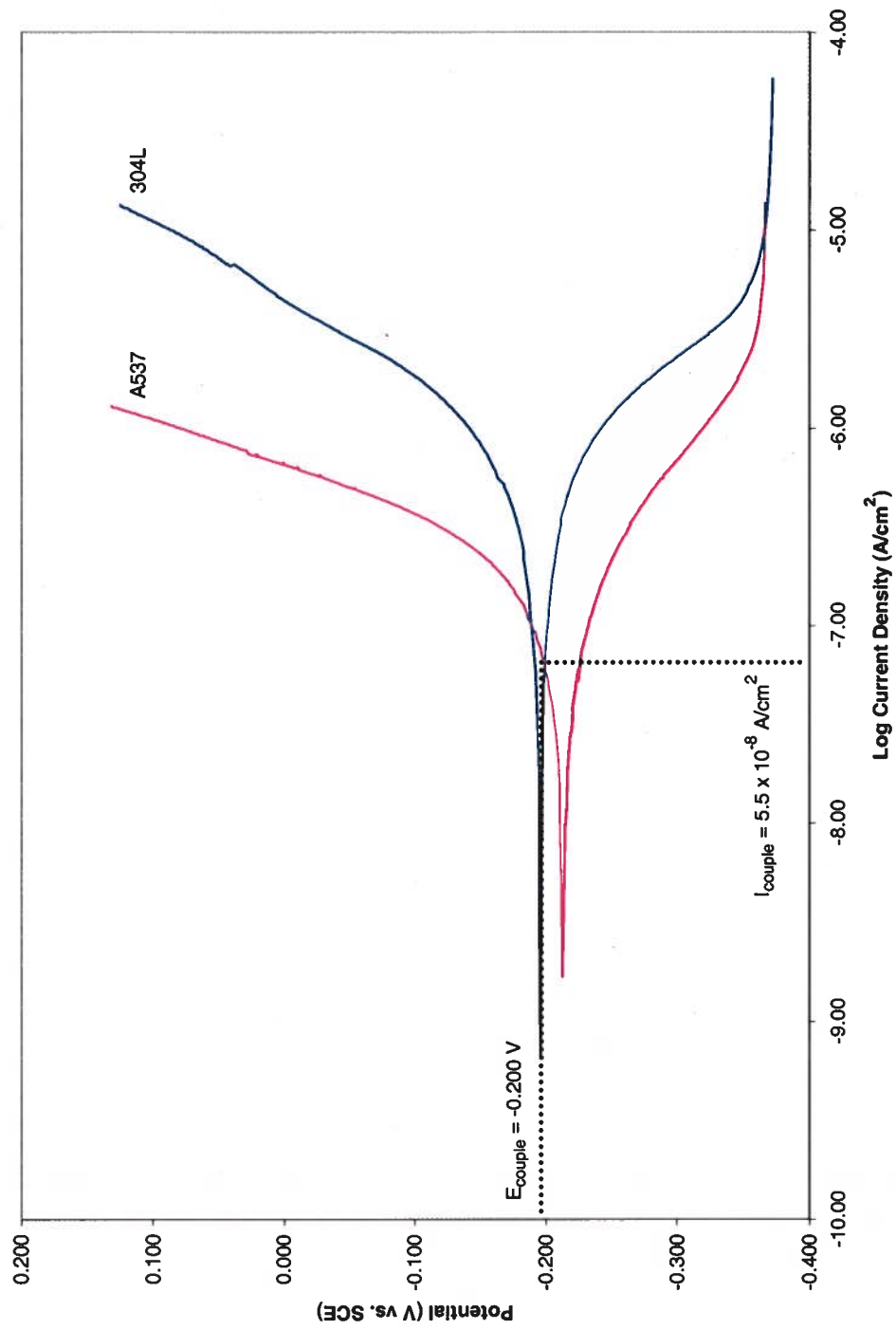


Figure 6. Overlay technique for waste simulant #9.

Distribution for WSRC-TR-2004-00580

T. M. Punch, 704-71F

M. Hubbard, 704-70F

C. A. McKeel, 730-1B

E. J. Freed, 703-H

D. J. Martin, 703-H

L. M. Fox, 703-H

N. C. Iyer, 773-41A

G. T. Chandler, 773-A

J. I. Mickalonis, 773-A

P. E. Zapp, 773-A